**Novel electrochemical synthesis of cellulose microfiber entrapped reduced graphene oxide: A sensitive electrochemical assay for detection of fenitrothion organophosphorus pesticide**

Vijayalakshmi Velusamy[a*†], Selvakumar Palanisamy[a,b**†], Shih-Wei Chen [b], Sridharan Balu[b], Thomas C.K. Yang[b***], Craig E. Banks[c]

[a]Division of Electrical and Electronic Engineering, School of Engineering, Manchester Metropolitan University, Chester Street, Manchester M1 5GD, United Kingdom

[b]Department of Chemical Engineering, National Taipei University of Technology, No. 1, Section 3, Chung-Hsiao East Road, Taipei City, Taiwan

[c]School of Science and Environment, Manchester Metropolitan University, Chester Street, Manchester M1 5GD, United Kingdom

Corresponding authors

* V. Velusamy (V.Velusamy@mmu.ac.uk)

** S. Palanisamy (prmselva@gmail.com)

*** T.C.K. Yang (ckyang@mail.ntut.edu.tw)

† These authors contributed equally

**Abstract**

Over the past decades, synthesis of carbohydrate polymers incorporated graphene or reduced graphene oxide has received greater attention in different disciplines owing to their unique physicochemical properties. In this context, we report a facile electrochemical synthesis of cellulose microfibers supported reduced graphene oxide and its application towards enhanced and lower potential electrochemical detection of fenitrothion. The synthesized cellulose microfibers supported reduced graphene oxide composite was further characterized using Fourier-transform infrared spectroscopy, Raman spectroscopy and high resolution scanning electron microscopy. Cyclic voltammetry studies reveal that cellulose microfibers supported reduced graphene oxide composite modified screen-printed carbon electrode exhibits a superior electro-reduction ability and lower reduction potential towards fenitrothion compared to screen-printed carbon electrodes modified with graphene oxide, graphene oxide-cellulose microfibers, and reduced graphene oxide. Furthermore, cellulose microfibers supported reduced graphene oxide composite modified electrode showed 141 mV lower reduction potential towards fenitrothion than the chemically reduced graphene oxide- cellulose microfibers composite modified screen-printed carbon electrode. The effect of accumulation time, catalyst loading, scan rate and pH for the detection of fenitrothion has been studied and discussed. Differential pulse voltammetric studies show that the fabricated composite electrode can detect the fenitrothion in a wider linear response range up to 1.134 mM with a detection limit of 8 nM. To validate the proof of concept, the fabricated sensor was successfully applied for the detection of fenitrothion in different water samples.

**Keywords:** Electrochemical reduction, reduced graphene oxide, cellulose microfibers, fenitrothion, electroanalysis

## 1. Introduction

In recent years, significant research has aimed at the synthesis of carbohydrate polymers incorporated carbon nanomaterials due to their improved physicochemical properties [**1, 2**]. In particular, the synthesis of carbohydrate polymers incorporated graphene oxide (GO) derivatives has received tremendous interest due to their novel applications in different areas including electrochemical sensing [**3-5**]. Reduced graphene oxide (RGO) is an inexpensive 2D carbon nanomaterial, widely used in different fields including electroanalysis due to its high conductivity, large surface area to volume ratio, excellent biocompatibility and superior electrochemical properties [**6-8**]. However, the stability of RGO is poor in aqueous solution due to the restacking of individual graphene sheets, thereby significantly limiting the unique properties of RGO [**9-11**]. To overcome this problem, different materials have been used to prevent the aggregation and to uphold the unique properties of RGO [**12**]. Furthermore, the range of micro and nanomaterials have been used to improve the physicochemical properties of RGO which include the carbon nanomaterials [**13, 14**], metal oxides/metal alloy nanoparticles [**15-18**], conducting polymers [**19, 20**], carbohydrate polymers [**5**]. These advanced composites have not only enhanced the surface area but also significantly improves the electrolyte-absorption properties and electrochemical conductivity of RGO.

Recent studies revealed that carbohydrate polymers incorporated RGO have shown higher stability and improved physicochemical properties than RGO [**21**]. For instance, chitosan [**22**], β-cyclodextrin [**22, 23**], and cellulose [**24**] incorporated RGO composites have shown more significant interest in the electrochemical sensors and biosensors due to their combined unique properties with RGO. Among different carbohydrate polymers, cellulose is the most abundant natural polymer and has been widely used as a promising base material for diverse applications due to its low cost, lightweight, high thermal stability, high adsorption capacity, and biocompatibility [**25, 26**]. In particular, cellulose microfibers (CMF) has the high surface area, high porosity, and can be easily integrated with conducting network such as RGO [**27**]. Our recent studies revealed that CMF effectively prevents the agglomeration of pristine graphene and forms the stable

composite for biosensor applications [**24**]. However, chemical or thermal reduction methods mostly have been used in the preparation of RGO based cellulose composites [**28-31**]. In addition, there are no reports available for the electrochemical preparation RGO/cellulose composites, and these composites never been used for electroanalysis/analytical applications. In this context, for the first time, we have synthesized CMF integrated RGO composite by a simple electrochemical reduction method and used as an electrode material for sensing of fenitrothion (FNTN). FNTN (O, O-dimethyl O-(3-methyl-4-nitrophenyl) phosphorothioate) is one of the organophosphorus pesticides, widely used for controlling against insects on vegetables, rice, stored grains, fruits, cotton, and cereals [**32**]. Organophosphorus pose a severe threat to the natural environment, human health and animals due to its high toxicity. Furthermore, they can easily have contaminated into food and water due to their readily available nature and routine use in commercial, domestic and industrial purposes [**33, 34**]. Hence, reliable monitoring of FNTN at its low levels is more important and is of interest. Compared with available polarographic and chromatographic methods, electrochemical methods are widely used for sensitive detection of FNTN due to their simplicity, low-cost and high sensitivity [**35**]. To date, a vast number of modified electrodes have been used for sensitive and reliable detection of FNTN including graphene-based composites [**32-37**]. However, the fabrication of highly sensitive sensors for precise determination of FNTN, with wide linear range and low detection limit, is of interest regarding environmental safety, food safety, and human health.

In the present work, we describe a novel electrochemical preparation of CMF supported RGO composite for the first time. The resulting composite modified electrode was used for the enhanced and lower-potential detection of FNTN. The unique physicochemical properties (strong absorption, excellent electron transfer ability, large surface area to volume ratio) of RGO-CMF composite results into the high sensitivity, lower detection limit and broader linear response range for the detection of FNTN. Furthermore, the fabricated sensor shows improved analytical performances toward FNTN than previously reported modified electrodes including RGO composites.

## 2. Experimental

### *2.1. Materials and method*

Screen printed carbon electrodes (geometric surface area = 0.079 $cm^2$) were purchased from Zensor R&D, Taiwan. Graphite flakes (98% purity) and cellulose microfibers (medium) were purchased from Sigma Aldrich, Taiwan. Fenitrothion (PESTANAL®, analytical standard) was obtained from Sigma-Aldrich, Taiwan. Sterile-filtered doubly distilled (DD) water was purchased from Sigma-Aldrich, UK. All other chemicals were obtained from Sigma-Aldrich, UK and used as received. The supporting electrolyte, 0.1 M phosphate buffer (pH 7.0) was prepared from 0.1 M $Na_2PO_4$, and $NaH_2PO_4$ in DD water and the pH was adjusted using either 0.1 M NaOH or $H_2SO_4$. Real samples (tap and drinking water) were collected from the Manchester Metropolitan University campus and were used as collected. All chemicals used in this work is of analytical grade and used without any purification or modification. All the experiments were conducted at ambient temperature (25 ± 2 °C) unless otherwise stated. Bransonic Ultrasonic Bath with an operating frequency of 40 kHz and ultrasonic power output of 250 W was for sonication.

Cyclic voltammetry and differential pulse voltammetry (DPV) experiments were carried out using EmStat USB powered potentiostat from PalmSens, The Netherlands. The electrochemical interface consisting of three electrode configuration, wherein the modified SPCE (active surface are = 0.122 $cm^2$) as working electrode and a thin Pt wire and Ag/AgCl as a counter and reference electrodes, respectively. The geometric surface area of the unmodified SPCE is 0.8 $cm^2$. Fourier-transform infrared spectroscopy (FTIR) measurements were carried out using a Thermo SCIENTIFIC Nicolet iS10 instrument. High-resolution scanning electron microscopy (SEM) images of the as-prepared materials were acquired using Hitachi S-4300SE/N High-Resolution Schottky Analytical VP scanning electron microscope. Raman spectroscopy studies were carried out using Dong Woo 500i Raman spectrometer.

### *2.2. Electrochemical synthesis of RGO-CMF composite*

The graphite oxide synthesized from natural graphite using the adopted Hummers method [**10**]. GO suspension (50 mL) was prepared by dispersing the obtained graphite oxide (1 mg $mL^{-1}$) into the water with the help of sonication about 30 min. Before electrochemical synthesis of RGO-CMF, the GO–CMF composite was prepared by dispersing graphite oxide (5 mg $mL^{-1}$) into the CMF solution using ultrasonication for approximately 30 min. The stable CMF solution was prepared by the addition of 10 mg $mL^{-1}$ of CMF into the DD water and sonicated for 45 min at 10 °C. About 8 µL of GO–CMF composite dispersion was dropped on SPCE and allowed to dry in an air oven. The GO–CMF modified electrode was transferred to $N_2$ saturated pH 7.0 and was then electrochemically reduced to RGO–CMF by performing continuous potential cycling (15 cycles) from 0 to −1.5 V at a scan rate of 50 mV $s^{-1}$ [**10**]. The resulting modified electrode is denoted as RGO–CMF. The RGO modified electrode also prepared by a similar method without CMF. The schematic representation for preparation of RGO–CMF, and RGO is shown in **Figure 1**. For comparison, the chemically reduced graphene oxide (CRGO)-CMF composite was prepared, in which the hydrazine hydrate was used as a reducing agent for GO-CMF composite. In brief, about 5 µL of hydrazine hydrate was added to the 10 mL of as-prepared GO-CMF suspension (5 mg $mL^{-1}$) and was stirred for 10 h at 80ºC. The resulting CRGO-CMF composite was filtered and dried in an air oven. Other modified electrodes such as GO and GO-CMF modified SPCEs were prepared by drop coating of 8 µL of GO and GO-CMF dispersion on SPCE. The FNTN and other chemical stock solutions were prepared using DD water. All electrolyte solutions were deoxygenated by purging the pure $N_2$ (3 min), and the experiments were conducted at ambient temperature (25 ± 2 °C) unless otherwise stated.

## 3. Results and discussion

*3.1. Characterizations*

High-resolution scanning electron microscopic images of GO, GO-CMF, and RGO is shown in **Figure 2**. **Figure 2A** shows the SEM image of GO and appears as a thin sheet-like morphology with a thickness of

a few nanometers as expected. Upon introduction of CMF, the morphology of GO changes to ultra-thin net-like morphology (**Fig. 2B**), which is due to the intramolecular hydrogen bonding between CMF and GO. Our previous studies have shown that the morphology of CMF is a dense fiber morphology [**24**]. On the other hand, the RGO-CMF composite (**Fig. 2C**) appears as a 3D thin porous morphology with few nanosheets folded together. This is due to the strong electron scattering by RGO-CMF than GO-CMF and enfolding of thin layers of CMF on the surface of RGO. It is evident from **Figure 2D** that CMF is attached on the semi-transparent RGO of the composite. It is worthy to note that the morphology of RGO-CMF composite was changed to the 3D lamellar structure when GO-CMF is electrochemically reduced. The unique morphological features and porous nature of RGO-CMF composite will provide more active sites for adsorption of FNTN and result into the improved electron transfer towards the electrode surface. On the other hand, the SEM image of CRGO-CMF composite shows a typical 2D wrinkled morphology. The result confirms the successful transformation of GO-CMF to RGO-CMF composite. The FTIR (**Figure S1A**) and Raman (**Figure S1B**) spectroscopic studies also confirmed the successful formation of RGO-CMF composite. The detailed explanations can be found in the Supporting Information.

*3.2. Electrochemistry of FNTN at RGO-CMF modified SPCE*

The electrocatalytic activity of different modified SPCEs towards the reduction of FNTN was investigated using cyclic voltammetry. **Figure 3** shows the cyclic voltammetric response of GO (a), GO-CMF (b), RGO (c), CRGO-CMF (d) and RGO-CMF (e) modified SPCEs in pH 7.0 containing 0.3 mM FNTN at a scan rate of 50 mV/s. It can be seen that GO modified SPCE did not show any distinct peak for FNTN. However, the GO-CMF shows a sharp reduction peak at -0.721 V for FNTN, due to the direct reduction of the nitro group of FNTN to hydroxylamine [**32**]. The result indicates that the electro-reduction ability has been greatly enhanced upon introduction CMF with GO. The enhanced electro-reduction ability of GO-CMF composite is may be due to the structural changes of GO upon introduction of CMF (**Figure 2B**), which resulted in more adsorption of FNTN on the GO-CMF electrode surface. On the other hand, RGO modified

electrode did not show a sharp reduction peak to FNTN, while it shows a broad reduction peak at -0.716 V. The observed electro-reduction peak current of FNTN is lower than those observed at GO-CMF modified electrode. The enhanced detection of FNTN at GO-CMF composite is due to the strong interactions of CMF with GO, and improve the adsorption of more FNTN on GO-CMF composite electrode. In contrast, RGO-CMF composite modified electrode shows a distinct and sharp reduction peak at -0.61 V for FNTN. Upon reverse scan, a sharp oxidation peak was observed at -0.086 V and is due to the oxidation of hydroxylamine to nitroso derivative. The observed reduction peak current response of FNTN at RGO-CMF composite electrode was 3 folds higher than those observed at GO and GO-CMF modified electrodes. The strong electrostatic interactions between the composite and FNTN are resulted in the enhanced sensitivity of FNTN on the composite electrode surface. It is interesting to note that the RGO-CMF modified electrode has similar electrocatalytic activity towards FNTN when compared with the response of CRGO-CMF modified electrode. In addition, the reduction peak potential of FNTN at RGO-CMF modified electrode was 116, 121 and 141 mV lower than RGO, GO-CMF and CRGO-CMF modified SPCEs. The enhanced reduction ability and lower reduction potential detection of FNTN at RGO-CMF composite are possibly due to the presence of unique morphological features (**Figure 2C**) and porous nature of RGO-CMF composite. Hence, RGO-CMF composite can be used as a sensitive modified electrode for lower potential detection of FNTN.

To optimize the drop coating amount of GO-CMF composite on SPCE, different amount of GO-CMF composite was coated on SPCE and electrochemically reduced to RGO-CMF composite. The resulting electrode was used for the detection of 0.3 mM of FNTN using cyclic voltammetry. The other experimental conditions are similar to **Figure 3**. The obtained results are shown in **Figure 3 inset**, and the result revealed that 8 µL drop coated electro-reduced GO-CMF composite has a maximum current response to FNTN than other drop coated electro-reduced GO-CMF composite. Moreover, the response was decreased when the drop coating of the composite was over or below 8 µL and hence, 8 µL drop coated electro-reduced GO-CMF composite modified SPCE was used as an optimum for further electrochemical experiments. The

specific electrochemical mechanism of FNTN at RGO-CMF composite electrode is shown in **Figure 4**. To further illustrate the electrochemical behavior of FNTN at RGO-CMF modified electrode, the effect of scan rate was studied against the reduction peak current response of 0.3 mM FNTN in pH 7.0 using cyclic voltammetry. **Figure 5A** shows the cyclic voltammetry response of RGO-CMF modified SPCE in pH 7.0 containing 0.2 mM FNTN at different scan rates, and the scan rates were tested in a range between 20 to 180 mV/s. The reduction peak current of FNTN increases with increasing the scan rate from 20 to 180 mV/s. In addition, the peak potential of FNTN slightly shifted towards negative direction upon sweeping the higher scan rates. It was found from **Figure 5B** that the cathodic peak current of FNTN has a linear relationship with scan rates from 20 to 180 mV/s with the correlation coefficient ($R^2$) of 0.9947. The result indicates that the electrochemical reduction of FNTN is typical adsorption controlled electrochemical process [**33**]. To further support this claim, the linear plot between log scan rate vs. log cathodic peak current was made, and the obtained slope value was 0.96. The result indicates that the electrochemical reduction of FNTN is controlled by an adsorption process since the slope value of 1.0 is expected for adsorption controlled and 0.5 is for diffusion-controlled processes. It is necessary to study the effect of the cathodic current response of FNTN in different accumulation time since the electrochemical reduction of FNTN at RGO-CMF composite was an adsorption-controlled process. The obtained results show that the cathodic peak current response of FNTN had reached its threshold when the accumulation time was 80 s and was stable when the accumulation time was over 80 s. Hence, an accumulation time of 80 s was used as an optimum for further quantitative measurements.

The effect of pH vs. cathodic peak current response of FNTN was studied using cyclic voltammetry. The cyclic voltammetry response of RGO-CMF modified SPCE in 0.3 mM FNTN containing different pHs were studied at a scan rate of 50 mV/s. The obtained results of the cathodic peak current response of FNTN in different pH (pH 3.0 to 11.0) were plotted in **Figure 5C**. The result shows that a maximum cathodic current response of FNTN was observed at pH 7.0 than another pH. The reason is may be due to the high stability

of the composite and abundant availability of protons for reduction of FNTN. It was noted that the RGO-CMF composite showed a reasonable sensitivity for FNTN at pH 6.0 and 8.0. The result reveals that RGO-CMF modified SPCE can be used in broader pH, which is more reliable for active detection of FNTN in real samples. However, pH 7.0 is used as an optimum for quantitative measurements.

*3.3. Analytical merits of the sensor*

DPV was used for the electrochemical determination of FNTN using RGO-CMF composite modified SPCE since DPV offers more sensitivity, lower analytical detection limit (pM) and better resolution than other electrochemical techniques such as cyclic voltammetry, linear sweep voltammetry, and amperometry. **Figure 6A** shows typical DPV response of RGO-CMF composite modified SPCE for the absence (a') and presence (a-k) of different concentrations of FNTN (0.03-1333.8 μM) into deoxygenated pH 7.0 with an accumulation time of 80 s. In the absence of FNTN, RGO-CMF composite modified electrode did not show the response in the potential sweep between 0.2 to -0.9 V, which shows that the modified electrode is electrochemically inactive in the absence of FNTN. However, a notable response was observed at -0.602 V for the presence of 30 nM FNTN (curve a), which reveals the electro-reduction of FNTN by the composite modified electrode. The DPV response increases with increasing the addition of FNTN (curve b to k) and 90% of steady state current after a perturbation reaches in 4 s. The result clearly shows that the RGO-CMF composite modified has the higher electro-reduction ability and fast response time towards FNTN. As shown in **Figure 6B**, the response of the sensor was linear from 0.03 to 1133.8 μM additions of FNTN into the pH 7.0 with the $R^2$ of 0.9941. The sensitivity of the sensor was 1.76 $\mu A \mu M^{-1}$ $cm^{-2}$ and was calculated from the slope of the calibration plot/electrochemically active surface area (0.122 $cm^2$) of the electrode. The limit of detection (LOD) of the sensor was 12 nM and was calculated using IUPAC recommendations. To further explore the novelty and advantages of RGO-CMF composite modified electrode, the analytical performances of the sensor is compared with the recently reported FNTN sensors. The comparative results are shown in Table ST1. The Table STI clearly revealed that the fabricated sensor electrode has superior analytical performances in terms

of low LOD (8 nM) and wider linear response ranges (up to 1133.8 mM) than recently reported peptide-nanotubes [**32**], cerium(IV) oxide/RGO [**33**], ruthenium phthalocyanine-silica/multi-walled carbon nanotubes [**34**], pretreated glassy carbon electrode [**35**], multiwalled carbon nanotubes [**36**] and $TiO_2$/nafion [**37**] based FNTN sensors. We have only made the comparison of the sensor with recently published reports since these electrode materials have shown superior electroanalytical performance towards FNTN than their formerly published literature. Hence, the fabricated RGO-CMF composite is more suitable and advanced electrode material for the sensitive and low-level detection of FNTN.

*3.4. Selectivity and practical applications*

To further explore the sensor for practical applications, the selectivity of the RGO-CMF composite modified electrode was evaluated in the presence of potentially interfering nitro compounds containing pesticides and organic molecules. The selectivity of the sensor was evaluated for the detection of 0.1 μM FNTN in the presence of 100-fold addition of nitrite (100 μM) and 50 fold additions (50 μM) of methyl parathion, nitrophenol (ortho and para), nitrobenzene, p-nitrotoluene, p-nitroaniline, phoxim, and imidacloprid. DPV was used to evaluate the selectivity, and the experimental conditions are similar to **Figure 6A**. The obtained results are shown in **Figure 6C**. It can be seen that the tested nitro compounds containing pesticides and organic molecules showed acceptable relative error (<8%) on the modified electrode towards detection of FNTN. The reason is possibly due to the presence of similar reactivity of nitro functional group on tested interfering compounds. While, the nitrite showed a less relative error (<3%) on the modified electrode, which revealed the high selectivity of the sensor. The results demonstrate that the RGO-CMF composite modified electrode can be used for selective detection of FNTN in the presence of tested interfering compounds.

The practicality of the RGO-CMF composite modified electrode was tested in FNTN containing different water samples. The tap and drinking water samples were used for detection of FNTN, and they were

FNTN free. Before analysis, the pH of both water samples was adjusted to pH 7.0. The known concentration (0.2 and 0.5 μM) of FNTN was added into the water samples and used for the real sample analysis. The recovery values were calculated using the standard addition method, and the recovery values are tabulated in **Table ST2**. It is evident from **Table ST2** that the average recovery of the sensor was 97.6 and 97.2% in tap and drinking water samples, respectively. Also, the sensor also shows appropriate repeatability with an average relative standard deviation of 2.6 and 2.9% for the detection of FNTN in tap and drinking water samples. The result confirmed that the fabricated sensor electrode could be used for the real-time detection of FNTN in tested water samples.

The temporal stability of the RGO-CMF modified electrode towards the detection of 1 μM FNTN was examined by DPV at different time intervals. The experimental conditions are similar to **Figure 6A**. The DPV cathodic peak current response of FNTN was monitored periodically up to 41 h, and the obtained stability results are shown in **Figure 6D**. It can be seen that the sensor retained 96.1 and 94.2% of the first sensitivity of FNTN after 15 and 41 h, which indicates the suitable storage stability of the developed sensor. The excellent durability of the sensor is attributed to the high stability of the RGO-CMF composite and strong adsorption of FNTN on the modified electrode.

## 4. Conclusions

A simple electrochemical method has been used for the preparation of RGO-CMF composite modified electrode for the first time, which replace the tedious chemical and thermal reduction methods. The FTIR, Raman spectroscopy and high-resolution scanning electron microscopic characterizations confirmed the formation of RGO-CMF composite. Voltammetric studies revealed that the fabricated composite modified electrode has higher sensitivity and lower reduction potential towards detection of FNTN than that of other modified electrodes including CRGO. The as-prepared FNTN sensor offers many advantages such as high sensitivity, lower LOD, more extensive response range, high stability, and appropriate selectivity. The high porosity, excellent conductivity and high adsorption ability of the composite have resulted in the high

sensitivity and low LOD for the detection of FNTN. The excellent recovery of FNTN in water samples revealed the potential ability of the developed sensor for practical applications. However, the selective detection of FNTN in the presence of high concentrations of nitro compounds would be difficult due to the presence of similar functional groups. As a future perspective, the RGO-CMF composite can be used as a potential electrode material for biosensor and energy storage applications owing to its discussed unique physicochemical properties.

## 5. Conflict of interest

The authors declare no competing financial interest.


## Acknowledgments

The work was supported by the Engineering and Materials Research Centre (EMRC), School of Engineering, Manchester Metropolitan University, Manchester, UK. This work also jointly sponsored by the Ministry of Science and Technology (project No: 106-2119-M-027-001) of Taiwan. Authors also acknowledge the Precision analysis and Materials Research Center, National Taipei University of Technology for providing the all necessary Instrument facilities.

**References**


[1] D. Liu, Y. Zhang, X. Sun, P.R. Chan, Recent advances in bio-sourced polymeric carbohydrate/nanotube composites, J. Appl. Polym. Sci., 131 (2014) 40359.

[2] F. Cheng, C. Liu, H.B. Li, X. Wei, T. Yan, Y. Wang, Y. Song, J. He, Y. Huang, Carbon nanotube-modified oxidized regenerated cellulose gauzes for hemostatic applications, Carbohydr. Polym. 183 (2018) 246-253.

[3] H. Liu, C. Liu, S. Peng, B. Pan, C. Lu, Effect of polyethyleneimine modified graphene on the mechanical and water vapor barrier properties of methyl cellulose composite films, Carbohydr. Polym. 182 (2018) 52-60.

[4] E. Bagheripour, A.R. Moghadassi, S.M. Hosseini, B.V. Bruggen, F. Parvizian, Novel composite graphene oxide/chitosan nanoplates incorporated into pes based nanofiltration membrane: chromium removal and antifouling enhancement, Ind. Eng. Chem. Res. 62 (2018) 311-320.

[5] T.D. Andreeva, S. Stoichev, S.G. Taneva, R. Krastev, Hybrid graphene oxide/polysaccharide nanocomposites with controllable surface properties and biocompatibility, Carbohydr. Polym. 181 (2018) 78-85.

[6] Y. Zhu, S. Murali, W. Cai, X. Li, J.W. Suk, J.R. Potts, R.S. Ruoff, Graphene and graphene oxide: synthesis, properties, and applications, Adv. Mater. 22 (2010) 3906–3924.

[7] Y. Wang, Z. Li, J. Wang, J. Li, Y. Lin, Graphene and graphene oxide: biofunctionalization and applications in biotechnology, Trends Biotechnol. 29 (2011) 205-212.

[8] S.J. Rowley-Neale, E.P. Randviir, S.S. Abo Dena, C.E. Banks, An overview of recent applications of reduced graphene oxide as a basis of electroanalytical sensing platforms, Appl. Mater. Today, 10 (2018) 218–226.

[9] C. Karuppiah, S. Palanisamy, S.M. Chen, V. Veeramani, P. Periakaruppan, A novel enzymatic glucose biosensor and sensitive non-enzymatic hydrogen peroxide sensor based on graphene and cobalt oxide nanoparticles composite modified glassy carbon electrode, Sens. Actuators, B 196 (2014) 450-456.

[10] B. Unnikrishnan, S. Palanisamy, S.M. Chen, A simple electrochemical approach to fabricate a glucose biosensor based on graphene–glucose oxidase biocomposite, Biosens. Bioelectron. 39 (2013) 70-75.

[11] R.Y.N. Gengler, A. Veligura, A. Enotiadis, E.K. Diamanti, D. Gournis, C. Jozsa, B.J.V. Wees, P. Rudolf, Large-yield preparation of high-electronic-quality graphene by a langmuir–schaefer approach, Small, 6 (2010) 35.

[12] V.B. Mohan, K. Lau, D. Hui, D. Bhattacharyya, Graphene-based materials and their composites: a review on production, applications and product limitations, Composites Part B, 142 (2018), 200-220.

[13] M. Fang, Z. Wang, X. Chen, S. Guan, Sponge-like reduced graphene oxide/silicon/carbon nanotube composites for lithium ion batteries, Appl. Surf. Sci., 436 (2018) 345-353.

[14] B. Thirumalraj, S. Palanisamy, S.M. Chen, C.Y. Yang, P. Periakaruppan, B.S. Lou, Direct electrochemistry of glucose oxidase and sensing of glucose at a glassy carbon electrode modified with a reduced graphene oxide/fullerene-C60 composite, RSC Adv., 5 (2015) 77651-77657.

[15] B. Vellaichamy, P. Prakash, A facile, one-pot and eco-friendly synthesis of gold/silver nanobimetallics smartened rGO for enhanced catalytic reduction of hexavalent chromium, RSC Adv., 6 (2016) 57380-57388.

[16] S.K. Ponnaiah, P. Prakash, B. Vellaichamy, A new analytical device incorporating a nitrogen doped lanthanum metal oxide with reduced graphene oxide sheets for paracetamol sensing, Ultrason. Sonochem. 44 (2018) 196-203.

[17] S. Palanisamy, S.M. Chen, R. Sarawathi, A novel nonenzymatic hydrogen peroxide sensor based on reduced graphene oxide/ZnO composite modified electrode, Sens. Actuators, B,166-167 (2012) 372-377.

[18] S. Palanisamy, C. Karuppiah, S. M. Chen, Direct electrochemistry and electrocatalysis of glucose oxidase immobilized on reduced graphene oxide and silver nanoparticles nanocomposite modified electrode, Colloids Surf. B, 114 (2014) 164-169.

[19] H, Al-Sagur, S. Komathi, M.A. Khan, A.J. Gurek, A. Hassan, A novel glucose sensor using lutetium phthalocyanine as redox mediator in reduced graphene oxide conducting polymer multifunctional hydrogel. Biosens. Bioelectron., 92 (2017) 638-645.

[20] B. Vellaichamy, P. Periakaruppan, S.K. Ponnaiah, A new in-situ synthesized ternary CuNPs-PANI-GO nano composite for selective detection of carcinogenic hydrazine, Sens. Actuators, B, 245 (2017) 156-165.

[21] M.L. Foresti, V.B. Boury, Applications of bacterial cellulose as precursor of carbon and composites with metal oxide, metal sulfide and metal nanoparticles: a review of recent advances, Carbohydr. Polym., 157 (2017) 447-467.

[22] C. Li, Z. Wu, H. Yang, L. Deng, X. Chen, Reduced graphene oxide-cyclodextrin-chitosan electrochemical sensor: effective and simultaneous determination of o- and p-nitrophenols, Sens. Actuators, B, 251 (2017) 446-454.

[23] W.N. Nyairo, Y.R. Eker, C. Kowenje, E. Zor, H. Bingol, A. Tor, D.M. Ongeri, Efficient removal of lead(ii) ions from aqueous solutions using methyl-β-cyclodextrin modified graphene oxide, Water Air Soil Pollut., 288 (2017) 406

[24] V. Velusamy, S. Palanisamy, S.M. Chen, T. Chen, S. Selvam, S.K. Ramaraj, B. Lou, Graphene dispersed cellulose microfibers composite for efficient immobilization of hemoglobin and selective biosensor for detection of hydrogen peroxide, Sens. Actuators, B, 252 (2017) 175-182.

[25] M. Maria, P. Madrigal, M.G. Edo, Powering the future: application of cellulose-based materials for supercapacitors, Green Chem., 18 (2016) 5930–5956.

[26] M. Pääkkö, J. Vapaavuori, R. Silvennoinen, H. Kosonen, M. Ankerfors, T. Lindström, L.A. Berglund, O. Ikkala, Long and entangled native cellulose i nanofibers allow flexible aerogels and hierarchically porous templates for functionalities, Soft Matt., 4 (2008) 2492–2499.

[27] S. Palanisamy, S.K. Ramaraj, S. M. Chen, T.C,K, Yang, P. Yi-Fan, T. Chen, V. Velusamy, S. Selvam, A novel laccase biosensor based on laccase immobilized graphene-cellulose microfiber composite modified screen-printed carbon electrode for sensitive determination of catechol, Sci. Rep., 7 (2017) 41214.

[28] K. Gao, Z. Shao, Z. Wu, X. Wang, j. Li, Y. Zhang, W. Wang, F. Wang, Cellulose nanofibers/reduced graphene oxide flexible transparent conductive paper, Carbohydr. Polym., 97 (2013) 243–251.

[29] J.T. Korhonen, M. Kettunen, R.H.A. Ras, O. Ikkala, Hydrophobic nanocellulose aerogels as floating, sustainable, reusable, and recyclable oil absorbents, ACS Appl. Mater. Interfaces, 3 (2011) 1813–1816.

[30] C. Zhang, R.Z. Zhang, Y.Q. Ma, W. B. Guan, X. L. Wu, X. Liu, H. Li, Y.L. Du, C.P. Pan, Preparation of cellulose/graphene composite and its applications for triazine pesticides adsorption from water, ACS Sustainable Chem. Eng., 3 (2015) 396–405.

[31] N.D. Luong, N. Pahimanolis, U. Hippi, J.T. Korhonen, J. Ruokolainen, L.S. Johansson, J. D. Namd, J. Seppala, J. Mater. Graphene/cellulose nanocomposite paper with high electrical and mechanical performances, J. Mater. Chem. 21 (2011) 13991–13998.

[32] G. Bolat, S. Abaci, T. Vural, B. Bozdogan, E.B. Denkbas, Sensitive Electrochemical detection of fenitrothion pesticide based on self-assembled peptide-nanotubes modified disposable pencil graphite electrode, J. Electroanal. Chem., 809 (2018) 88-95.

[33] A.A. Ensafi, R. Noroozi, N.Z. Atashbar, B, Rezaei, Cerium(IV) oxide decorated on reduced graphene oxide, a selective and sensitive electrochemical sensor for fenitrothion determination, Sens. Actuators, B, 245 (2017) 980-987.

[34] T.C. Canevari, T. M. Prado, F. H. Cincotto, S. A.S. Machado, Immobilization of ruthenium phthalocyanine on silica-coated multi-wall partially oriented carbon nanotubes: electrochemical detection of fenitrothion pesticide, Mater. Res. Bull., 76 (2016) 41-47.

[35] W. Geremedhin, M. Amare, S. Admassie, Electrochemically pretreated glassy carbon electrode for electrochemical detection of fenitrothion in tap water and human urine, Electrochim. Acta, 87 (2013) 749-755.

[36] A. Kumaravel, M. Chandrasekaran, A Biocompatible nano $TiO_2$/nafion composite modified glassy carbon electrode for the detection of fenitrothion, J. Electroanal. Chem., 650 (2011) 163-170.

[37] H. Salehzadeh, M. Ebrahimi D.; Nematollahi, A.A. Salarian, Electrochemical study of fenitrothion and bifenox and their simultaneous determination using multiwalled carbon nanotube modified glassy carbon electrode, J. Electroanal. Chem., 767 (2016) 188–194.

**Figure captions**

**Figure 1:** Schematic representation of the preparation of RGO–CMF, and RGO.

**Figure 2:** SEM images of GO (A), GO-CMF (B), RGO-CMF (C) and CRGO-CMF (D).

**Figure 3:** Cyclic voltammetry response of SPCE modified with GO (a), GO-CMF (b), RGO (c), CRGO-CMF (d) and RGO-CMF composite (e) in deoxygenated pH 7.0 containing 0.3 mM FNTN at a scan rate of 50 mV/s. The inset shows the effect of drop coating amount of RGO-CMF composite vs. cyclic voltammetric electro-reduction peak current response of 0.3 mM FNTN. Error bar is relative to 3 measurements.

**Figure 4:** Proposed electrochemical mechanism of FNTN at RGO-CMF modified electrode.

**Figure 5:** A) Cyclic voltammetry response of RGO-CMF modified SPCE in pH 7.0 containing 0.2 mM FNTN at different scan rates from 20 to 180 mV/s. B) Linear calibration plot for scan rate vs. electro-reduction peak current response of FNTN. C) Effect of pH vs. electro-reduction peak current response of FNTN and the experimental conditions are similar to Fig. 3. Error bar is relative to 5% standard error.

**Figure 6:** A) DPV response of RGO-CMF composite modified SPCE for the absence (a') and presence of different concentrations of FNTN (a-k) into deoxygenated pH 7.0. B) The corresponding linear plot for [FNTN] vs. $I_{pc}$. Error bar is relative to 3 measurements. C) The selectivity of the RGO-CMF modified electrode towards detection of 0.1 µM FNTN for the presence of 20 fold additions of interfering species including nitro compounds and dihydroxybenzene isomers. D) Stability of the FNTN sensor up to 41 hours and the error bar is relative to 5% standard error. The experimental conditions for Fig. 6C and D are similar to Fig. 6A.

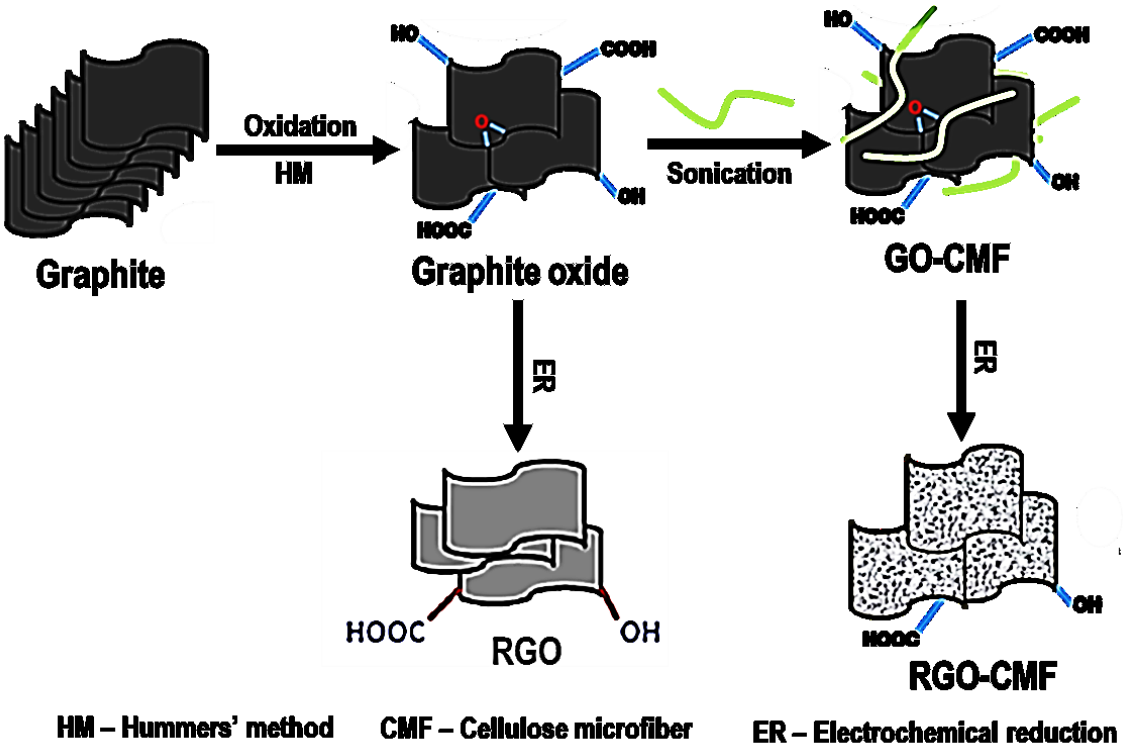
Graphite
Oxidation
HM
HO
COOH
O
OH
HOOC
Graphite oxide
Sonication
GO-CMF
ER
RGO
RGO-CMF
HM – Hummers' method
CMF – Cellulose microfiber
ER – Electrochemical reduction

Figure 1

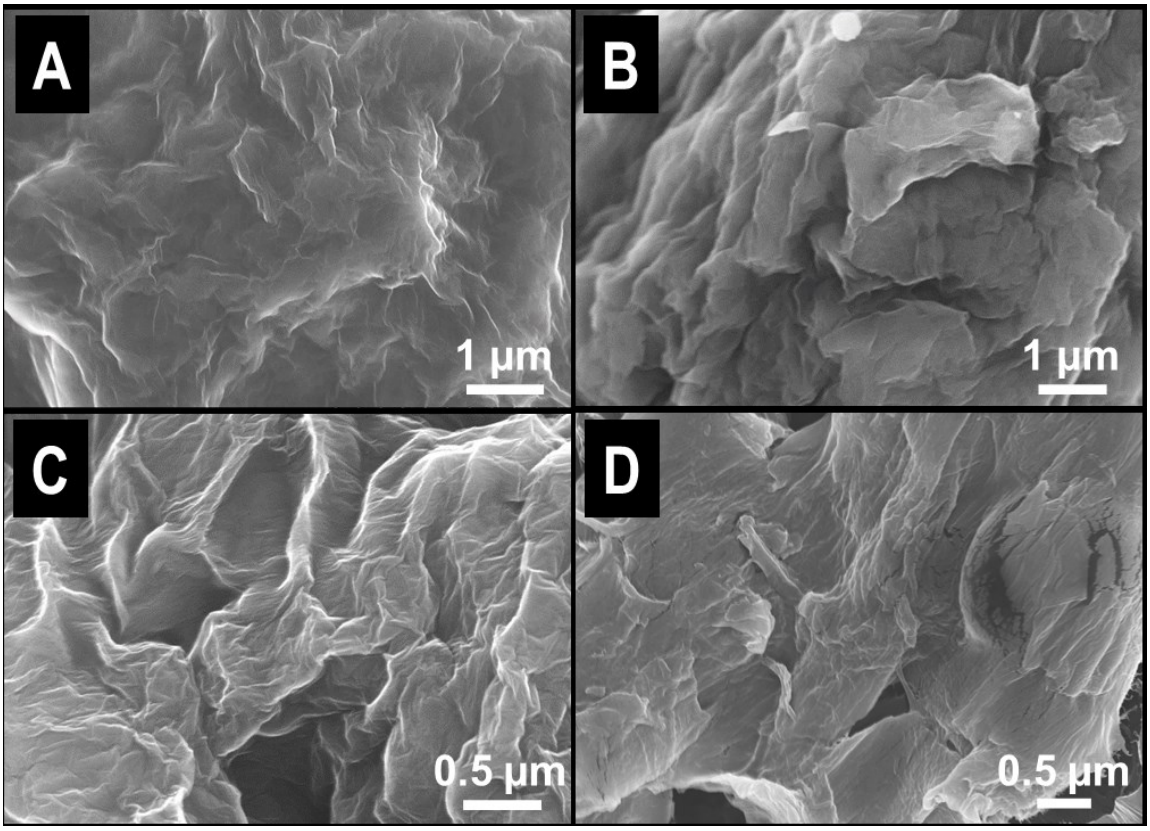


**Figure 2**

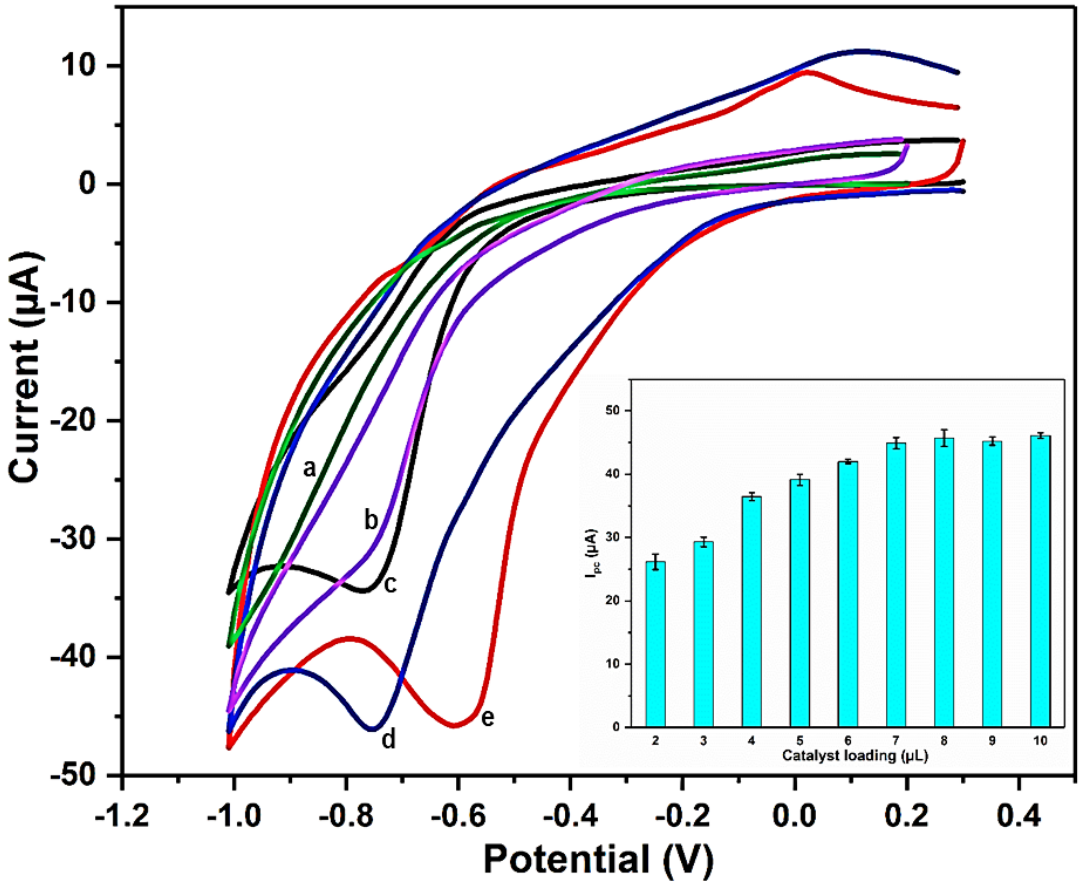
Current (μA)
Potential (V)
10
0
-10
-20
-30
-40
-50
-1.2
-1.0
-0.8
-0.6
-0.4
-0.2
0.0
0.2
0.4
a
b
c
d
e
$I_{pc}$ (μA)
Catalyst loading (μL)
0
10
20
30
40
50
2
3
4
5
6
7
8
9
10

**Figure 3**

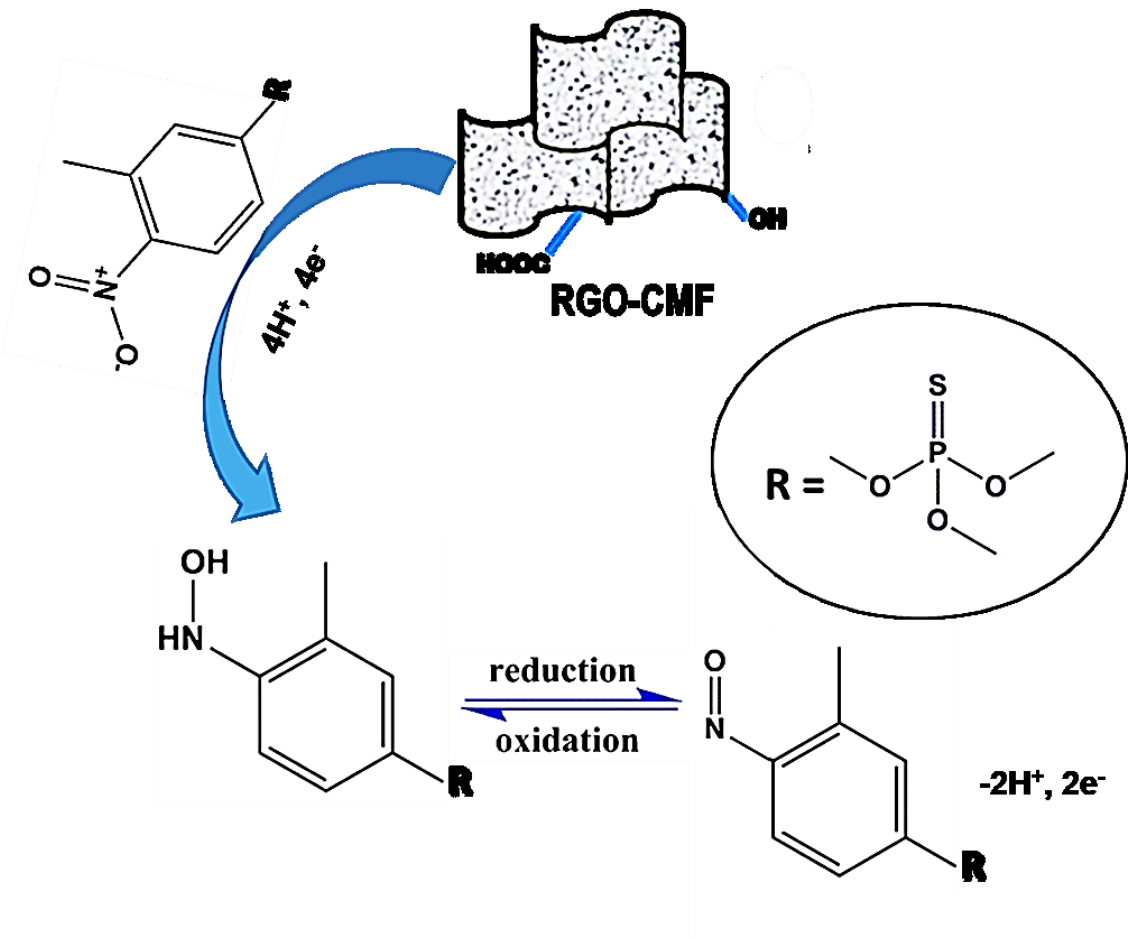
R
O
N+
O-
4H+, 4e-
OH
HOOC
RGO-CMF
S
R =
P
O
O
O
OH
HN
reduction
oxidation
R
O
N
-2H+, 2e-
R

Figure 4

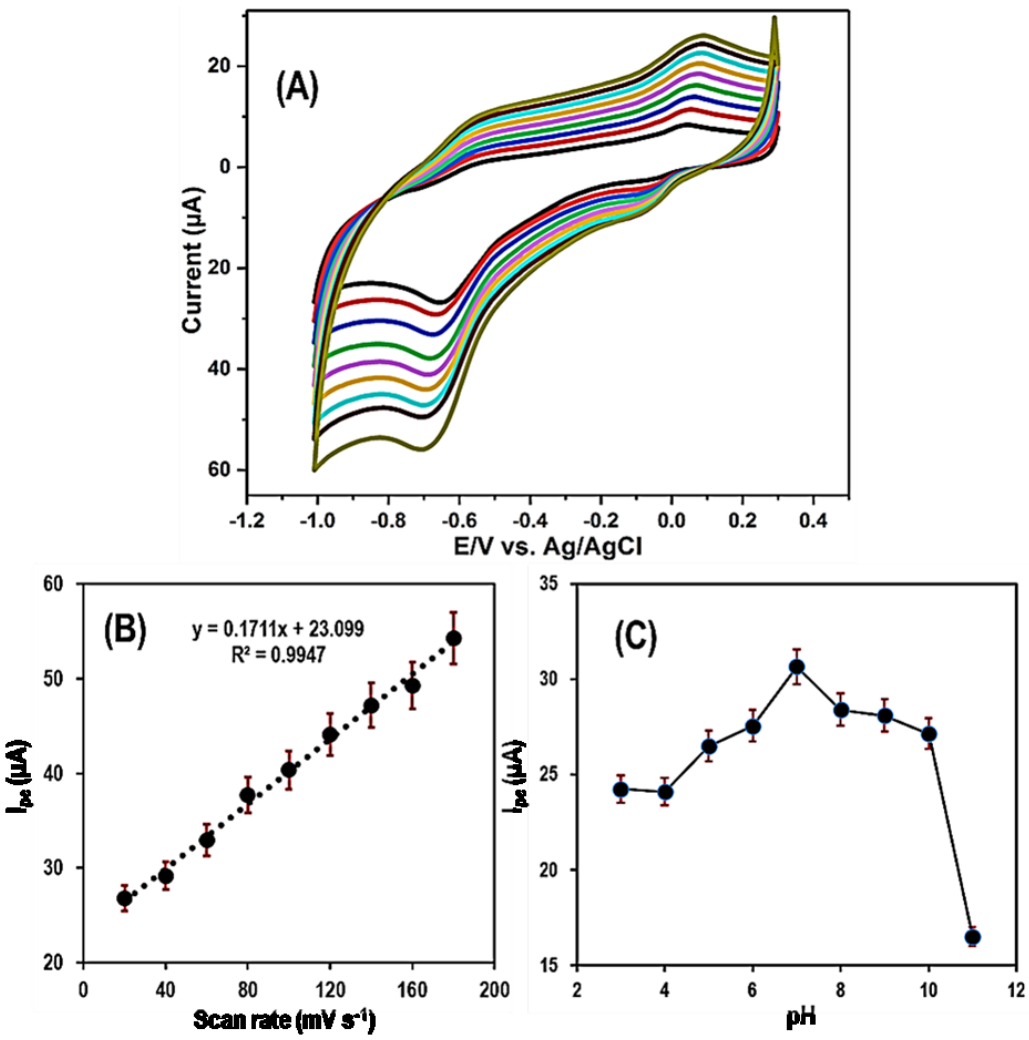
(A)
Current (μA)
E/V vs. Ag/AgCl
(B)
y = 0.1711x + 23.099
R² = 0.9947
Ipc (μA)
Scan rate (mV s-1)
(C)
Ipc (μA)
pH

**Figure 5**

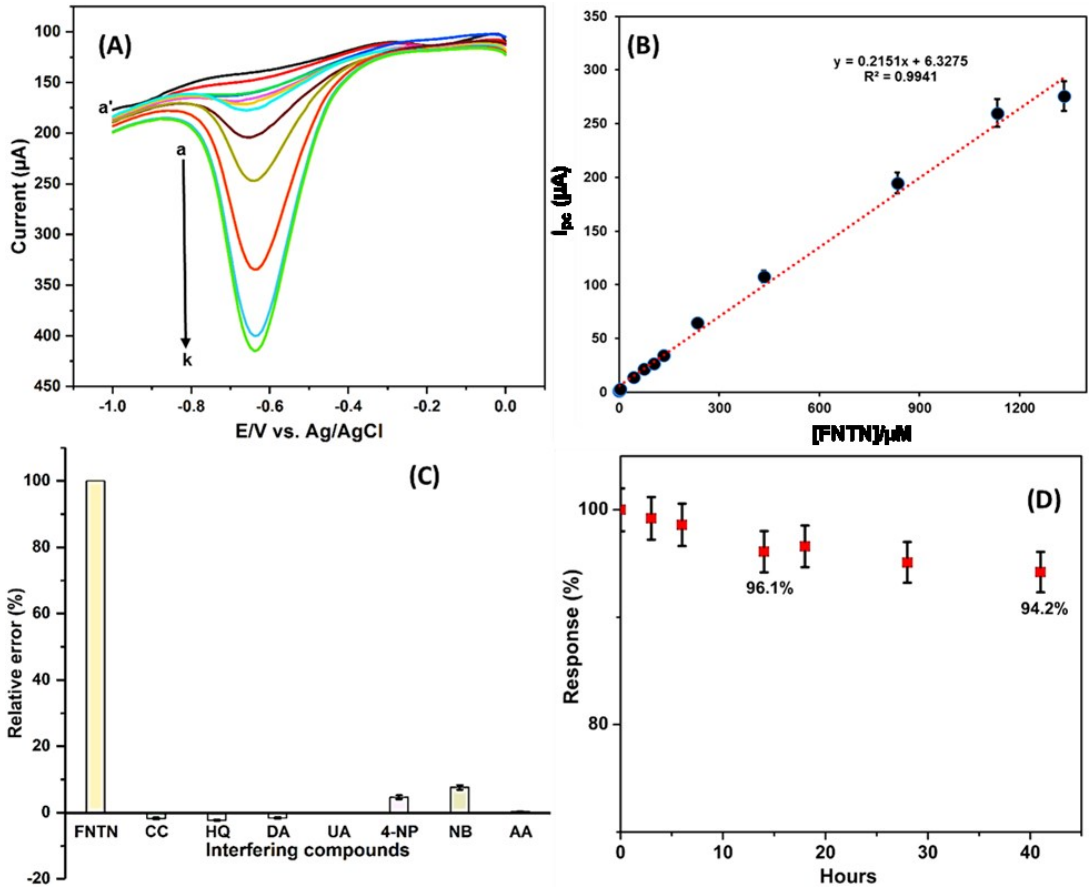
(A)
a'
a
k
Current (μA)
E/V vs. Ag/AgCl
(B)
y = 0.2151x + 6.3275
R² = 0.9941
[FNTN]/μM
(C)
Relative error (%)
FNTN
CC
HQ
DA
UA
4-NP
NB
AA
Interfering compounds
(D)
Response (%)
96.1%
94.2%
Hours

**Figure 6**

## TOC & Highlights